Marshall University

Marshall Digital Scholar

Weisberg Division of Engineering Faculty Research

Weisberg Division of Engineering

1-1-2015

Intelligent control of miniature holonomic vertical take-off and landing robot

Mohammad A. Jaradata

Mohamed Al-Fandia

Omar Alkhatiba

Yousef Sardahi

Journal of Intelligent & Fuzzy Systems 29 (2015) 1209–1217
DOI:10.3233/IFS-151721
IOS Press

Intelligent control of miniature holonomic vertical take-off and landing robot

Mohammad A. Jaradat[a,b,*], Mohamed Al-Fandi[a], Omar Alkhatib[a] and Yousef Sardahi[a]
[a]*Department of Mechanical Engineering, Jordan University of Science and Technology, Irbid, Jordan*
[b]*Department of Mechanical Engineering, American University of Sharjah, Sharjah, UAE*

Abstract. This paper discusses the development of a fuzzy based controller for miniaturized unmanned aerial vehicle (UAV).This controller is designed to control the center-of-gravity (CoG) in a new configuration of coaxial miniaturized flying robot (MFR). The idea is to shift the CoG by controlling two pendulums located in perpendicular directions; each pendulum ends with a small mass. A key feature of this work is that the control algorithm represents the original nonlinear function that describes the dynamics of the proposed system. The controller model incorporates two cascaded subsystems: PD and PI fuzzy logic controllers. These two controllers regulate the attitude and the position of the flying robot, respectively. A model of the proposed controllers has been developed and evaluated in terms of stability and maneuverability. The results show that the presented control system can be used efficiently for the MFR applications.

Keywords: UAV, MFR, VTOL, nonlinear modeling, nonlinear control

1. Introduction

Unmanned aerial vehicles (UAVs) in general and Vertical Take-off and Landing vehicles (VTOL) in particular have become vital platforms in many applications, such as exploration purposes, ground attacks and civil engineering tasks [4, 6, 7] because of their unique characteristics. These special traits include the ability to take-off and land vertically from unprepared sites, fly at low altitudes, and hover and maneuver in tightly constrained environments. Furthermore, UAVs are less costly [1–5]. In fact, UAVs are more advantageous than manned aircrafts in missions that are dangerous for crewmembers or those that are impossible for manned aircrafts because of their large size [8, 9]. As a result, there has been a considerable amount of interest in developing palm size vehicles that are able to navigate and perform simple missions using micro and/or nano components.

*Corresponding author. Mohammad A. Jaradat. Tel.: +96 2272 01000-22568; E-mail: majaradat@just.edu.jo.

In the literature, different controller schemes that autonomously controlled the UAV have been introduced. Some of these controllers were based on neural networks [10], fuzzy systems [11, 12], a hybrid combination of fuzzy methods and neural networks [13], PID controllers [14], adaptive controllers [15, 16] or genetic algorithms [17, 18]. In particular, the topic of vertical taking-off and landing was addressed by numerous research groups [4, 19–21]. In this context, different steering concepts were evaluated such as using swash plates to apply cyclic pitch to the rotor blades [22], using flaps to change the orientation of the down wash [18] or to displace the CoG [23]. The last mechanism has many advantages, including simplifying the mechanical design of the flying system and freedom of servo motor placement [21, 24]. Hence, CoG has been utilized as a successful steering mechanism in many growing investigations of MFR [23, 24]. In this research, a steering mechanism that depends on the displacement the CoG of MFR is discussed.

However, the actual nonlinear models that describe the real behavior of the UAV using the CoG steering technique is not been addressed yet. Most of the presented nonlinear control systems were applied on linearized models. Since UAVs are highly nonlinear, a nonlinear control system is needed. Therefore, a fuzzy logic control system has been developed to automate the vertical taking-off and landing phases of a flying robot. This control system applies an intelligent control technique to a redesigned coaxial MFR as will be described in forthcoming sections. In fact, the novelty of the proposed controller resides in developing a cascaded structure consisting of PD-fuzzy logic controller and PI-fuzzy logic controller. This cascaded control system is designed and implemented on a realistic nonlinear model of a real unmanned helicopter platform; the Newton-Euler model. The main core of this control system is the steering subsystem that consists of two controlled pendulums moving in perpendicular directions. Each pendulum ends with a small mass, which by changing the position of each pendulum, leads to a change in the total center of gravity (CoG).

Ultimately, to validate the performance of the configured CoG control mechanism, a real-time experiment, where, the experimental flight emphasizes the capability of such configuration to steer the robot in a per-defined direction based on CoG shifting.

2. Dynamics of the flying mechanism

2.1. System platform

The first goal of this research is to design a miniature flying coaxial robot platform. Figure 1 shows the proposed robot model. This system consists of two main sub systems: the coaxial subsystem and the steering/control subsystem. The coaxial subsystem is responsible of the hovering mechanism; it uses two contra rotating rotors to compensate each other's torque. The control subsystem consists of two controlled pendulums, one in the x-direction and the other in the y-direction. Each pendulum ends with a small mass. By changing the positions of the two masses, the total center of gravity of the flying system is changed. In other words, by controlling the positions of the two pendulums masses, the center of gravity of the flying system varies, thereby affecting the flying system by a controlling torque. Sequentially, this torque changes the attitude of the system. Two micro-servo motors were used to drive the two pendulums masses simultaneously to achieve the desired holonomic motion.

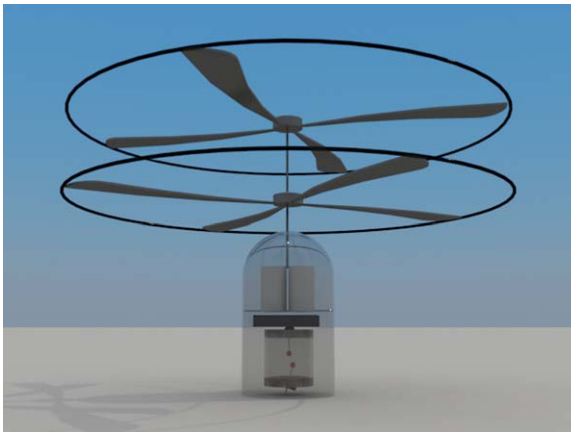

Fig. 1. Coaxial flying robot layout with CoG steering mechanism.

2.2. Mathematical model

In this paper, the controllers are developed based on a general nonlinear dynamic model of the flying robot system. In this model, the robot position is defined by the vector $\xi = [x,\ y,\ z]^T$, the robot rotation is defined by an orthogonal rotation matrix ${}^A_B R$: $R_A \to R_B$, where $R_B = \{X_B,\ Y_B,\ Z_B\}$ is the system frame, $R_A = \{X_A,\ Y_A,\ Z_A\}$ is the world frame and $R \in SO^{(3)}$. The orientation of the robot represented by the three Euler angles: yaw, pitch and roll angles denoted by $\eta = [\gamma\ \beta\ \alpha]^T$, respectively. The general coordinate for the flying robot is given by $q = [\xi\ \eta] \in R^{(6)}$.

$$
{}^A_B R(\eta) = R_z(\gamma) \cdot R_y(\beta) \cdot R_x(\alpha)
= \begin{bmatrix} c\gamma c\beta & c\gamma s\beta s\alpha - s\gamma c\alpha & c\gamma s\beta c\alpha + s\gamma s\alpha \\ s\gamma c\beta & s\gamma s\beta s\alpha + c\gamma c\alpha & s\gamma s\beta c\alpha - s\alpha c\gamma \\ -s\beta & c\beta s\alpha & c\beta c\alpha \end{bmatrix} \quad (1)
$$

The free body diagram of the proposed flying system is illustrated in Fig. 2. It includes the main forces applied by the flying system: the system's weight, the total lift force generated by the two rotors and the total force applied by the pendulums to the flight system. When the position of CoG changes, a torque is produced, which in turn changes the roll, pitch and yaw angles. As a result, the attitude and the velocity of the whole flying robot system change accordingly.

The rigid body dynamics of the robot's fixed frame can be represented using the general Newton-Euler model [25].

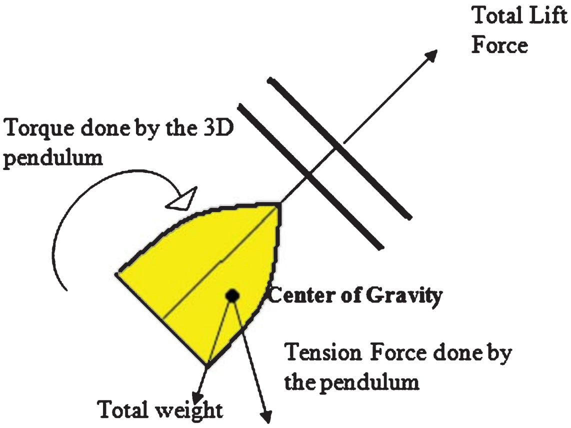

Fig. 2. A free body diagram for the proposed flying system.

$$\begin{bmatrix} mI_{3\times 3} & 0 \\ 0 & I \end{bmatrix} \ddot{q} + \begin{bmatrix} \dot{\eta} \times m\,\varsigma \\ \dot{\eta} \times I\dot{\eta} \end{bmatrix} = \begin{bmatrix} F \\ \tau \end{bmatrix} \quad (2)$$

Where, m is the mass of the body, I is the identity matrix, q is the acceleration of the center of mass, F is the total force acting on the center of mass and τ is the total torque acting about the center of mass. According to the frame shown in Fig. 2, the full translational and rotational dynamic model for an inertial fixed frame is given by [2, 25, 26]

$$\vec{F}_{on.system} = -m_c \begin{bmatrix} -2g.s\beta + \vec{a}_{Xball.net} \\ 2g.c\beta s\alpha + \vec{a}_{Yball.net} \\ 2g.c\beta c\alpha + \vec{a}_{Zball.net} \end{bmatrix} + \begin{bmatrix} 0 \\ 0 \\ 2C_T\Omega^2 \end{bmatrix} \quad (4)$$

The ball pendulum acceleration is given by Equation 5:

$$\vec{a}_{bal\ln et} = \vec{a}_{ball.C} + \vec{a}_{ball.D} = \begin{bmatrix} \ddot{x}_{system} \\ \ddot{y}_{system} + b\left(c\theta\ddot{\theta}\right) \\ \ddot{z}_{system} + b\left(c\theta\dot{\theta}^2\right) \end{bmatrix} + \begin{bmatrix} \ddot{x}_{system} + b\left(-c\phi\ddot{\phi}\right) \\ \ddot{y}_{system} \\ \ddot{z}_{system} + b\left(-s\phi\ddot{\phi} + c\phi\dot{\phi}^2\right) \end{bmatrix} \quad (5)$$

The produced total torque consists of the following: the torque generated by the lift force of the two rotors, as illustrated in Equation 6 and the torque resulting from the control subsystem due to a position change of CoG, as shown in Equation 7. The CoG is shifted through appropriate control commands according to two pendulum angles Φ and θ. Then, a net torque is generated, representing the difference of each rotor, as shown in Equation 8.

$$\begin{aligned}
\ddot{x} &= (c\beta c\gamma)\frac{1}{m}\left(\vec{F}_{on.system.X}\right) + (s\alpha s\beta c\gamma \;\; c\alpha s\gamma)\frac{1}{m}\left(\vec{F}_{on.system.Y}\right) + (c\alpha s\beta c\gamma + s\alpha s\gamma)\frac{1}{m}\left(\vec{F}_{on.system.Z}\right) \\
\ddot{y} &= (s\gamma c\beta)\frac{1}{m}\left(\vec{F}_{on.system.X}\right) + (s\alpha s\beta s\gamma + c\alpha c\gamma)\frac{1}{m}\left(\vec{F}_{on.system.Y}\right) + (c\alpha s\beta s\gamma \;\; s\alpha c\gamma)\frac{1}{m}\left(\vec{F}_{on.system.Z}\right) \\
\ddot{z} &= (\;\; s\beta)\frac{1}{m}\left(\vec{F}_{on.system.X}\right) + (s\alpha c\beta)\frac{1}{m}\left(\vec{F}_{on.system.Y}\right) + (c\alpha c\beta)\frac{1}{m}\left(\vec{F}_{on.system.Z}\right) \\
\ddot{\alpha} &= \dot{\beta}\dot{\gamma}\left(\frac{I_y \;\; I_z}{I_x}\right) \;\; \frac{J_r}{I_x}\dot{\beta}\Omega + \frac{1}{I_x}(M_total_in_X_direction) \\
\ddot{\beta} &= \dot{\alpha}\dot{\gamma}\left(\frac{I_z \;\; I_x}{I_y}\right) + \frac{J_r}{I_y}\dot{\alpha}\Omega + \frac{1}{I_y}(M_total_in_Y_direction) \\
\ddot{\gamma} &= \dot{\alpha}\dot{\beta}\left(\frac{I_x \;\; I_y}{I_z}\right) + \frac{1}{I_z}(M_total_in_Z_direction)
\end{aligned} \quad (3)$$

Where, $F_{on.system}$ is the total force applied on the system, M_{total} denotes the total moment that affects the system and $\vec{F}_{onsystem}$ represents the summation of the exerted force from the pendulums on the flying mechanism plus the total force produced by the robot rotors.

$$\tau_1 = \begin{bmatrix} -g\left(m_c b \sin\theta\right) \\ g\left(m_c b \sin\phi\right) \\ 0 \end{bmatrix} \quad (6)$$

$$\tau_2 = r_c \times \vec{F}_{P.on.system.C} + r_d \times \vec{F}_{P.on.system.D}$$
$$= -m_c b \begin{bmatrix} c\theta\,(\vec{a}_{Yball.C} + g.c\beta s\alpha) + s\phi\,(\vec{a}_{Zball.D} + g.c\beta c\alpha) + c\phi\,(\vec{a}_{Yball.D} + g.c\beta s\alpha) \\ -s\theta\,(\vec{a}_{Zball.C} + g.c\beta c\alpha) - c\theta\,(\vec{a}_{Xball.C} - g.s\beta) - c\phi\,(\vec{a}_{Xball.D} - g.s\beta) \\ s\theta\,(\vec{a}_{Yball.C} + g.c\beta s\alpha) - s\phi\,(\vec{a}_{Xball.D} - g.s\beta) \end{bmatrix} \quad (7)$$

$$\tau_3 = \vec{Q}_1 - \vec{Q}_2 = \begin{bmatrix} 0 \\ 0 \\ Q_1 - Q_2 \end{bmatrix} \quad (8)$$

Thus, the total system's dynamics are governed by the aerodynamic, gyroscopic, inertial torque and gravitational effects. While, the translational and rotational motions depend on the generated commands from the control subsystems.

3. Flying mechanism intelligent controllers

Most miniature vertical takeoff and landing robots (MVTLR) are maneuvered by controlling their attitude angles: roll, pitch, and yaw. These flight controllers mainly consist of two cascaded controller subsystems: an attitude controller that has a fast transient response time in order to serve the fastest system dynamics and a translational controller that controls with the slower system dynamics [11]. This separation of the control system has many advantages [30]. Firstly, it is appropriate for UAVs control due to their model mechanism. Secondly, the resulted control scheme is not complicated and it can be implemented and tuned easily. Finally, this separation of the control system has been used for many years in many aerospace applications such as spacecraft, launchers, aircraft, and UAVs, and the obtained results were acceptable. A block diagram of the proposed flight controller of the MVLTR is shown in Fig. 3. As shown in this diagram, the inner subsystem controller's inputs are the desired attitude angles $(\alpha,\ \beta,\ \gamma)_d$ and the outputs are the servo-motor control commands $(\theta,\ \varphi)$. The outer subsystem controller takes the desired position of the MVTLR $P_d = [x_d\ y_d\ z_d]^T$ as input and generates the desired attitude angles $(\alpha,\ \beta,\ \gamma)_d$ that produce the final desired position.

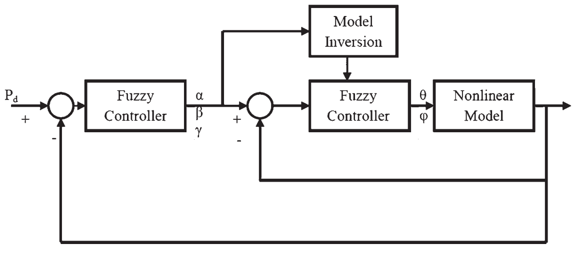

Fig. 3. Flight controller design.

3.1. Inner loop subsystem control

The inner loop subsystem control was mainly developed based on a fuzzy logic PD controller since its transient response is fast. The PD fuzzy control action (U) is represented as shown in Equation 9 [27–29]:

$$U = h \times Defuzzification \{R\,(Fuzzifitaction\,(g_0 \times e, g_1 \times \Delta e))\} \quad (9)$$

where, g_0, g_1 and h are the scaling gain factors. This system is mainly composed of the expert fuzzy If-Then rule base (R) that partitions the universe of discourse of the input variables: the error (e) and change in the error (Δe).

$$e = \begin{bmatrix} \alpha_d - \alpha \\ \beta_d - \beta \\ \gamma_d - \gamma \end{bmatrix} \quad (10)$$

A common format for the expert fuzzy If-Then rule base which describes the system's dynamics is as follow [28, 29]:

$$R_n : If\ e\ is\ A_i\ AND\ \ \Delta e\ is\ B_j\ Then\ u\ is\ C_{ij}$$

Where, A, B and C are the fuzzy linguistic variables that partition the inputs and output universe of discourses. Each linguistic variable is specified by a membership function μ, this function provides the input/output variables with its truth value $\mu_{Ai}(e) : R \to [0\ 1]$ for $i = 1, \ldots,\ n$, where n is the fuzzy membership functions' number for the input fuzzy variable e. The input variables were divided into five linguistic terms [Negative big (Nb), Negative small (Ns), zero (Z), Positive small (Ps), and Positive big (Pb)]. Each

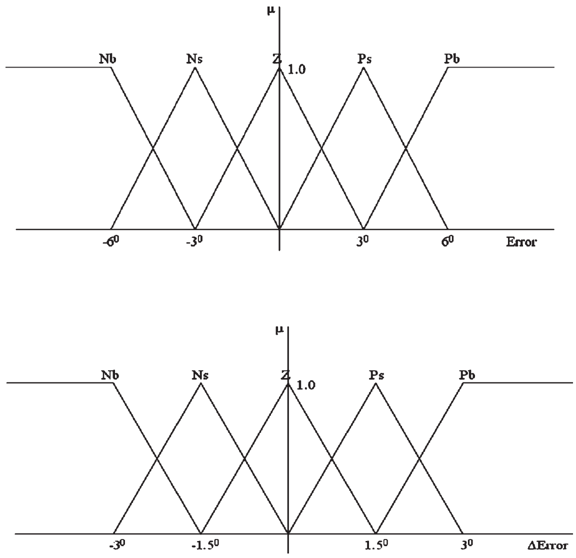

Fig. 4. Membership functions for the inputs of the inner loop.

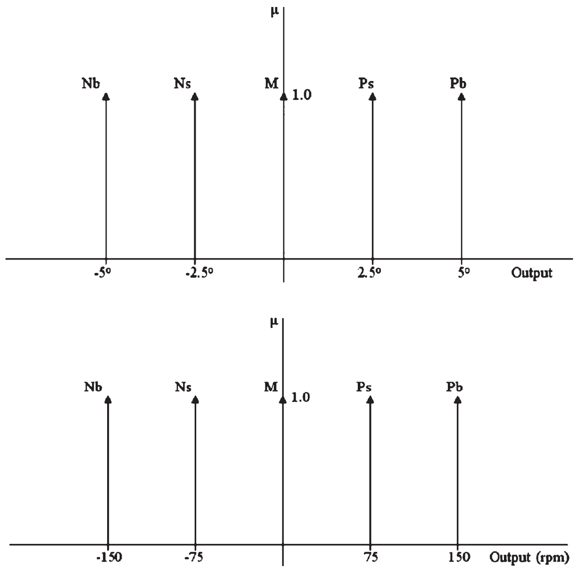

Fig. 5. Membership function for the output of the inner loop $U = [\theta\ \varphi\ \Omega_{diff}]^T$.

linguistic term was represented by triangular membership as illustrated in Equation 11 [27]. The partitioned universe of discourse for the input variables is shown in Fig. 4.

$$\forall e \in \Re : \mu_{A_i}(e) = \begin{cases} \max\left\{0, 1 + \frac{e-c_i}{0.5w_i}\right\} & if\ e \le c_i \\ \max\left\{0, 1 + \frac{c_i-e}{0.5w_i}\right\} & otherwise \end{cases} \tag{11}$$

Five linguistic terms for the fuzzy controller output variable were adapted: Negative big (Nb), Negative small (Ns), Medium (M), Positive small (Ps) and Positive big (Pb). These linguistic terms were represented by crisp membership as depicted in Equation 12 [27]. The partitioned universe of discourse for the input variables is shown in Fig. 5.

$$\forall u \in \Re : \mu_{c_i}(u) = \begin{cases} 1\ if\ u = \delta_i \\ 0\ otherwise \end{cases} \tag{12}$$

The set of rules which maps the expert knowledge into the input/output state spaces is shown in Table 1. This set of rules describes the system's dynamics as a multi-input-single-output (MISO) control system. The contribution of each rule can be generally represented as a fuzzy relation defined by Equation 13 [27], based on the t-norm operator.

Table 1
The inner control subsystem's fuzzy rules

U		e				
		Nb	Ns	Z	Ps	Pb
Δe	Nb	Pb	Pb	Ps	Ps	Medium
	Ns	Pb	Ps	Ps	Medium	Ns
	Z	Ps	Ps	Medium	Ns	Ns
	Ps	Ps	Medium	Ns	Ns	Nb
	Pb	Medium	Ns	Ns	Ns	Nb

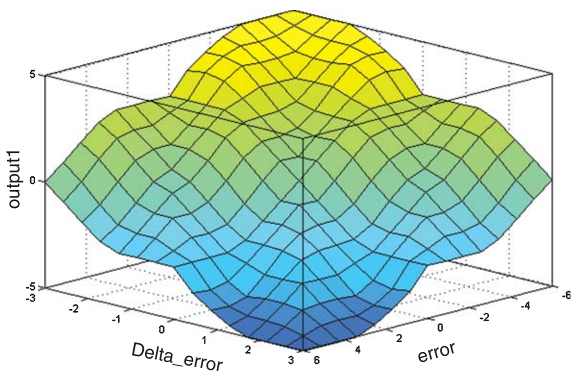

Fig. 6. Fuzzy control surface.

$$\forall n : R_n : u_n = \int_{e\times\Delta e} t(\mu_{A_i}(e), \mu_{B_j}(\Delta e))/(e, \Delta e) \tag{13}$$

The accumulated output fuzzy set based on the whole expert rules is given by Equation 14 utilizing Mamdani min-max t-norm/co-norm operators as an inference engine.

$$\mu(u) = \bigcup_{k=1}^{n} R_k = \bigcup_{k=1}^{n} \mu_k(e \cap \Delta e) o R_k(u), \tag{14}$$

The center of area was used as a deffuzzification method as in Equation 15 [27–29]. In this equation, $\mu(u)$ is the accumulated output as indicated before. By the deffuzzification, the output of the controller becomes a single real value U_c.

$$U_c = \frac{\int_u u\mu(u)du}{\int_u \mu(u)du} \tag{15}$$

3.2. Outer loop subsystem control

The outer loop subsystem control was mainly developed based on a fuzzy logic PI controller. It is well-know that this controller is accurate since it eliminates the steady-state error. The output of the control system in this case can be expressed by the following equation [27–29]:

$$\begin{aligned} \delta u &= Defuzzification \\ &\quad \{R\,(Fuzzifitaction\,(g_0 \times e, g_1 \times \Delta e))\} \\ u &= u_{i-1} + h \times \delta u \end{aligned} \tag{16}$$

Where, δu is the inferred change in the fuzzy controller output and u is the accumulated control action. The input state variables; the error e and the change in the error Δe, were defined in Equation 17 for a given reference position vector P_d.

$$e = P_d - P \tag{17}$$

A common format of the expert fuzzy If-Then rule base, which describes the PI dynamics, is as follows:

$$R_n : If\ e\ is\ A_i\ AND\ \ \Delta e\ is\ B_j\ Then\ \delta u\ is\ C_{ij}$$

The set of fuzzy linguistic variables A, B and C that partition the inputs/output universe of discourse by the fuzzy sets during fuzzification with each term membership function μ are shown in Figs. 7 and 8. The same convention is used as in the inner loop controller subsystem.

The set of rules that describes the relation between the inputs and the output fuzzy variables is shown in

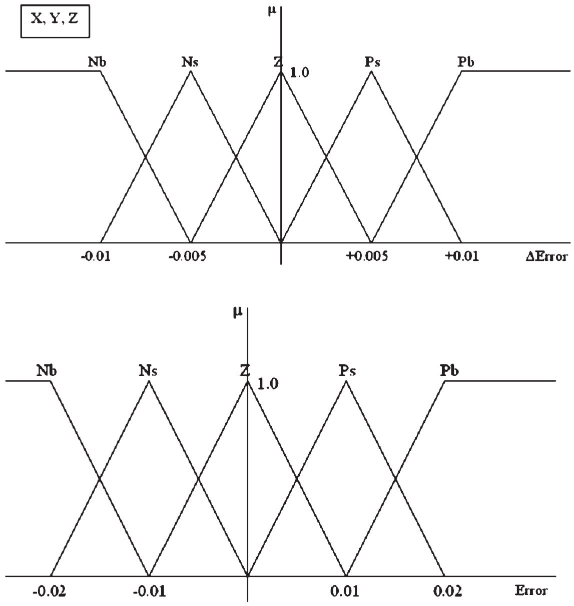

Fig. 7. Membership functions for the inputs of the outer loop.

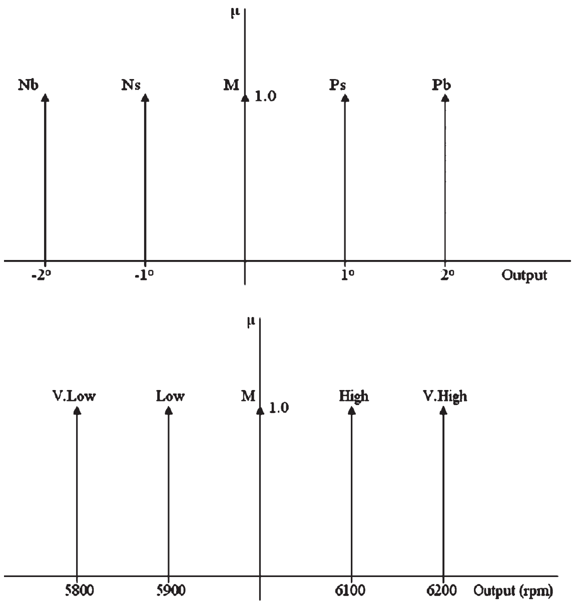

Fig. 8. Membership function for the output of the outer loop $\delta u = [\alpha\ \beta\ \Omega]^T$.

Table 2. The control surface, which depicts this relation, is shown in Fig. 9. As explained in this figure, this relationship is nonlinear, which is one of the attractive advantages of the fuzzy controllers, in particular when the controlled system is nonlinear. As in the inner control system, the accumulated output fuzzy

Table 2
Fuzzy rules of the outer controller subsystem

δu		e				
		Nb	Ns	Z	Ps	Pb
Δe	Nb	Pb	Pb	Ps	Ps	Zero
	Ns	Pb	Ps	Ps	Zero	Ns
	Z	Ps	Ps	Zero	Ns	Ns
	Ps	Ps	Zero	Ns	Ns	Nb
	Pb	Zero	Ns	Ns	Nb	Nb

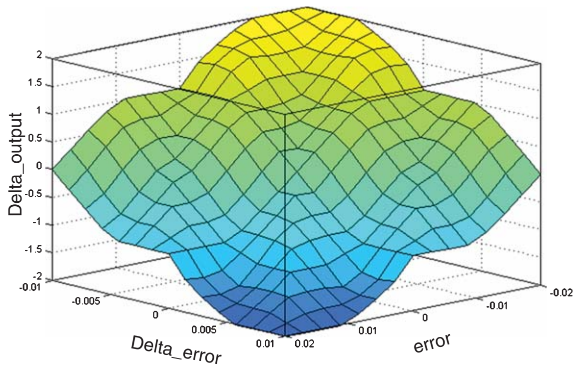

Fig. 9. Fuzzy control surface.

set, which is based on the expert rules, was inferred using Mamdani min-max t-norm/co-norm operators as an inference mechanism. In addition, the final crisp value of the controller was extracted using the center of area as a defuzzifier operator.

Finally, a model inversion was designed to provide an appropriate rotational speed for each rotor (Ω_1, Ω_2) based on the inferred Ω and Ω_{diff} control values form the outer and inner subsystems, respectively, as explained in Equation 18.

$$\Omega_1 = \frac{\Omega + \Omega_{diff}}{2}$$
$$\Omega_2 = \frac{\Omega - \Omega_{diff}}{2} \tag{18}$$

4. Results and discussions

A trajectory in a form of three-dimensional motion is selected as in Fig. 10. The goal of this test is to prove the ability of the controller to follow a path and, at the same time, maintain a constant heading. In addition, the sharp corners of the square path would induce a step-like response of the system for observation.

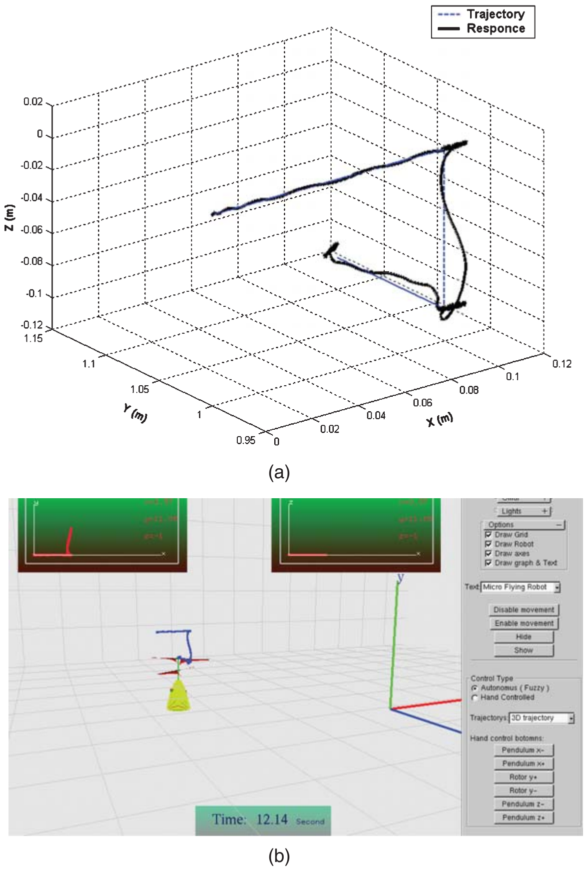

Fig. 10. Response of the flying robot in a three dimensional predefined path.

In this three-dimensional diagram, it is shown that the proposed flying system can change its direction easily, Fig. 11. In this evaluation test, the response of the inner control subsystem is shown in Fig. 12. In this Figure, the dashed line represents the desired attitude angles, which are generated by the outer control system. As shown, the inner loop dynamic was fast. The position of CoG was determined by θ and φ commands as shown in Figs. 12 and 13. From Fig. 12, it should be noted that the position of the center of gravity is similar to that of the system motion; however, it varies in two-dimensional planes.

5. Conclusions

This paper proposed a new design approach of a fuzzy flight control system. This closed-loop system controls a configured unmanned MFR. The developed controller was implemented on a general nonlinear

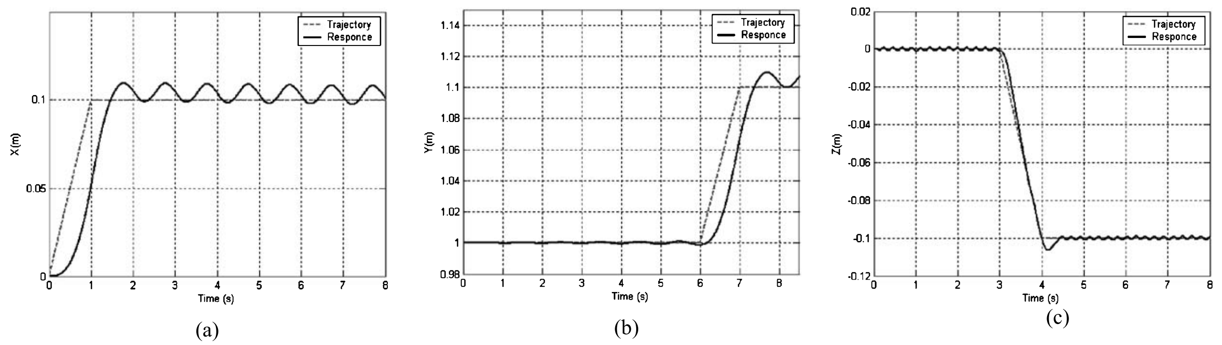

Fig. 11. The flying robot's response in the: (a) X-direction, (b) Y-direction, (c) Z-direction.

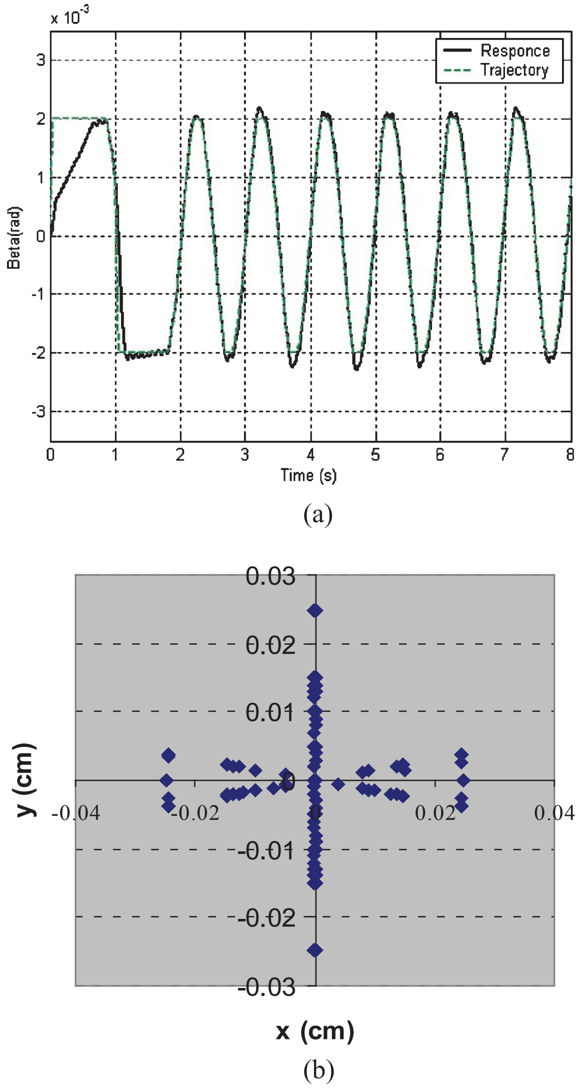

Fig. 12. (a) Attitude with time, the dashed line represents the desired angle. The solid line represents the actual angle (β) with time, (b) Center of gravity position.

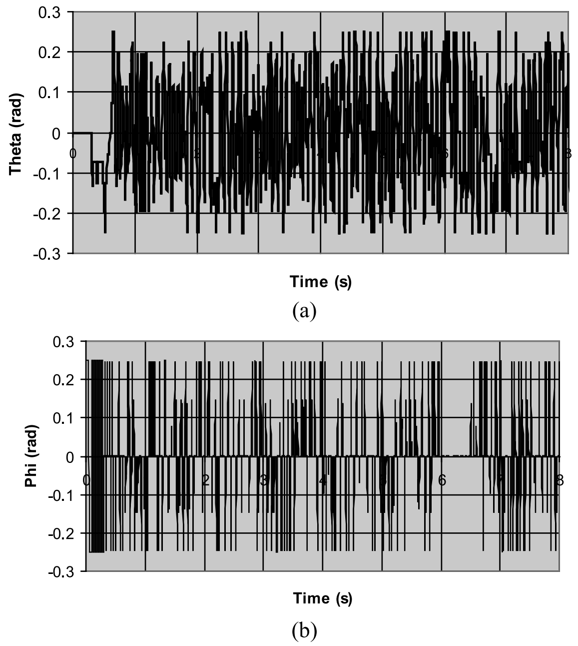

Fig. 13. (a) θ- action through the 3D motion, (b) φ- action through the 3D motion.

dynamic model of the flying system and examined in extensive simulations. The results demonstrated that the controller was stable and robust against external disturbances and was able to achieve aggressive flying. In particular, if the position of CoG changes, then the flying system is effected by a new torque that changes the attitude (γ, β, α). Consequently, there will be no need for the swash plate mechanism and hence, that will simplify the mechanical design. Most importantly, it has been proven that the nonlinear fuzzy controller makes the system stable in a wide range of situations. In addition, the controller exhibits robust behavior against external disturbances, where the system can track curvilinear trajectories with an excellent settling time and overshoot values. Ultimately, it can be inferred that the proposed controller, accompanied with the new MFR design, have the potential to achieve excellent performance for indoor applications.

References

[1] McKerrow, Li Chen and Phillip, Modelling the Lama Coaxial Helicopter, in Australasian Conference on Robotics & Automation, 2007.

[2] J. Escareño, A. Sanchez, O. Garcia and R. Lozano, Modeling and global control of the longitudinal dynamics of a coaxial convertible mini-UAV in hover mode, *Journal of Intelligent Robot System* **54** (2009), 261–273.

[3] D. Schafroth, C. Bermes, S. Bouabdallah and R. Siegwart, Modeling and system identification of the muFly micro helicopter, *Journal of Intelligent Robot System* **57** (2010), 27–47.

[4] S. Bouabdallah, P. Murrieri and R. Siegwart, Towards autonomous indoor micro VTOL, *Autonomous Robots* **18** (2005), 171–183.

[5] A. Rango, A. Laliberte, J.E. Herrick, C. Winters and K. Havstad, Development of an Operational UAV/Remote Sensing Capability for Rangeland Management, *in 23rd International UAV Systems Conference*, 2008.

[6] D. Vissiere, P.-J. Bristeau, A.P. Martin and N. Petit, Experimental autonomous flight of a small-scaled helicopter using accurate dynamics model and low-cost sensors, *in Proceedings of the 17th World Congress*, Seoul, Korea: The International Federation of Automatic Control, 2008.

[7] S.M. Ettinger, M.C. Nechyba, P.G. Ifju and M. Waszak, Vision-Guided Flight Stability and Control for Micro Air Vehicles, *Advanced Robotics* **17** (2003), 617–640.

[8] B. Mettler, *Identification Modeling and Characteristics of Miniature Rotorcraft*, Kluwer Academic, Springer US, 2003.

[9] Floreano, Jean-Christophe Zufferey and Dario, Toward 30-gram Autonomous Indoor Aircraft: Vision-based Obstacle Avoidance and AttitudeControl, *in Proceedings of the IEEE International Conference on Robotics and Automation*, 2005.

[10] Cangelosi, Fabio Ruini and Angelo, Extending the Evolutionary Robotics approach to flying machines: An application to MAV teams, *Newral Networks* **22** (2009), 812–821.

[11] B. Kadmiry and D. Driankov, A fuzzy flight controller combining linguistic and model-based fuzzy control, *Fuzzy Sets and Systems* **146** (2004), 313–347.

[12] SeferKurnaz, Omer Cetin and OkyayKaynak, Fuzzy logic based approach to design of flight control and navigation tasks for autonomous unmanned aerial vehicles, *Journal of Intelligent and Robotic Systems* **54** (2009), 229–244.

[13] K. Santa, S. Fatikow and G. Felso, Control of microassembly-robots by using fuzzy-logic and neural networks, *Computers in Industry* **39**(3) (1999), 219–227.

[14] S. Bouabdallah, A. Noth and R. Siegwart, PID vs. LQ Control Techniques Applied to an Indoor Micro Quadrotor, *in Proceedings of the IEEE International Conference on Intelligent Robots and Systems*, 2004.

[15] E.N. Johnson and S.K. Kannan, Adaptive trajectory control for autonomous helicopters, *AIAA J Guid Control Dyn* **28**(3) (2005), 524–538.

[16] SeferKurnaz, Omer Cetin and Okyay Kaynak, Adaptive neuro-fuzzy inference system based autonomous flight control of unmanned air vehicles, *Expert Systems with Applications* **37** (2010), 1229–1234.

[17] J.-C. Zufferey, D. Floreano, M. van Leeuwen and T. Merenda, Evolving Vision-Based Flying Robots in Biologically Motivated Computer Vision. Springer: Berlin/Heidelberg, 2010, pp. 13–29.

[18] T.T.H Ng and G.S.B. Leng, Design optimization of rotary-wing micro air vehicles proceedings of the institution of mechanical engineers, *Part C: Journal of Mechanical Engineering Science* **220**(6) (2006), 865–873.

[19] S. Bouabdallah, P. Murrieri and R. Siegwart, Design and Control of an Indoor Micro Quadrotor, *in IEEE International Conference on Robotics and Automation*, 2004.

[20] K. Mullens, A. Burmeister, M. Willsa, T. Nelson and T. Denewiler, Development of a UGV-Mounted Automated Refueling System for VTOL UAVs, *in SPIE Unmanned Systems Technology Conference VIII*, Orlando, FL, 2006.

[21] C. Bermes, K. Sartori, D. Schafroth, S. Bouabdallah and R. Siegwart, Control of a Coaxial Helicopter with Center of Gravity Steering, *in Intl Conf On Simulation, Modeling And Programming For Autonomous Robots*, 2008.

[22] D. Schafroth, S. Bouabdallah, C. Bermes and R. Siegwart, From the test benches to the first prototype of the muFly micro helicopter, *Journal of Intelligent and Robotic Systems* **54** (2009), 245–260.

[23] S. Bouabdallah, R. Siegwart and G. Caprari, Design and Control of an Indoor Coaxial Helicopter. *in Proceedings of the 2006 IEEE International Conference on Intelligent Robots and Systems*, Beijing, China, 2006.

[24] C. Bermes, S. Leutenegger, S. Bouabdallah, D. Schafroth and R. Siegwart, New Design of the Steering Mechanism for a Mini Coaxial Helicopter. *in IEEE/RSJ International Conference on Intelligent Robots and Systems*, Nice, France, 2008.

[25] P. Castillo, R. Lozano and A. Dzul, ed. Modelling and Control of Mini-Flying Machines. Series in Advances in Industrial Control. Springer-Verlag: New York, 2005.

[26] R. Siegwart and S. Bouabdallah, Towards Intelligent Miniature Flying Robots, in Field and Service Robotics. Springer Berlin/Heidelberg, 2006.

[27] K. Passino and S. Yarkovich, Fuzzy Control. Adisson-Wisley Longman, 1998.

[28] C. Lee, Fuzzy logic in control systems: Fuzzy logic controller–part I, *IEEE Transactions on Systems, Man, and Cybernetics*, 1990.

[29] C. Lee, Fuzzy logic in control systems: Fuzzy logic controller–part II, *IEEE Transactions on Systems, Man, and Cybernetics*, 1990.

[30] F. Kendoul, I. Fantoni and R. Lozan, Asymptotic Stability of Hierarchical Inner-Outer Loop-Based Flight Controllers. *Proceedings of the 17th World Congress, the International Federation of Automatic Control*, Seoul, Korea, 2008.